Available online at www.sciencedirect.com

ScienceDirect

Procedia Engineering 103 (2015) 237 – 245

Procedia Engineering

www.elsevier.com/locate/procedia

The 13th Hypervelocity Impact Symposium

Strength of Granular Materials in Transient and Steady State Rapid Shear

Ryan C. Hurley[a], José E. Andrade[a]*

[a]*California Institute of Technology, Pasadena, CA 91125, USA*

Abstract

This paper discusses relationships between the frictional strength of a flowing granular material and quantities including porosity and grain-scale energy dissipation. The goal of the paper is to foster an understanding of frictional strength that will facilitate the development of constitutive laws incorporating important physical processes. This is accomplished in several steps. First, a friction relationship is derived for a steady state simple shear flow using an energy balance approach. The relationship shows that friction is explicitly related to porosity, grain connectivity, and grain-scale dissipation rates. Next, the friction relationship is extended to describe transient changes in frictional behavior. The relationship shows that, in addition to the processes important for steady flows, the rate of dilatation and changes in internal energy play a role in the frictional strength of a granular material away from steady state. Finally, numerical simulations are performed to illustrate the accuracy of the friction relationships and illuminate important scaling behavior. The discussion of numerical simulations focuses on the rate-dependence of frictional strength and the partition of macroscopic energy dissipation into its grain-scale components. New interpretations of existing constitutive laws and ideas for new constitutive laws are discussed.

Peer-review under responsibility of the Curators of the University of Missouri On behalf of the Missouri University of Science and Technology

Keywords: Granular flow, rheology, friction, strength

Nomenclature

I	the inertial number, a non-dimensional shear rate equal to $\dot{\gamma}d/\sqrt{P/\rho_g}$
d	characteristic grain size or grain diameter for spherical grains
P	confining pressure
ρ_g	grain density
ϕ	solid fraction
Z	coordination number, average number of contact points per grain
U_c	elastic emerged stored at grain contact
T_p	kinetic energy of grain
Greek symbols	
$\dot{\gamma}$	shear rate in simple shear or strain rate tensor in 3D
β	rate of dilatation
Γ_c	dissipation rate at grain contact
μ	friction coefficient
μ_{ss}	steady state portion of the friction coefficient
μ_t	transient portion of the friction coefficient
μ_n	portion of the friction coefficient furnished by grain viscoelasticity

* Corresponding author. Tel.: 626-395-4141

E-mail address: jandrade@caltech.edu.

Peer-review under responsibility of the Curators of the University of Missouri On behalf of the Missouri University of Science and Technology

doi:10.1016/j.proeng.2015.04.032

μ_s	portion of the friction coefficient furnished by grain sliding

1. Introduction

The behavior of flowing granular media has long been of interest in the engineering and physics communities. Researchers in these fields have sought to identify the numerical schemes and material properties required to accurately model dense and rapid granular flows in various scenarios. Such scenarios include powder transport [1], rapid soil penetration [2], the flow of brittle ceramics [3], and planetary-scale asteroid impact [4]. A diverse set of modeling techniques has emerged to address this diverse set of application. For instance, discrete element modeling [5] and its multi-physics variants [6] have been used for applications in which only hundreds or thousands of grains need to be modeled. Rate-dependent plasticity theories, kinetic gas theories, and Navier-Stokes solvers have been reserved for field-scale modeling [7]. This latter set of continuum approaches is the only computationally tractable means of modeling many problems and remains a prime focus of on-going research. In these approaches, material strength is captured by a friction coefficient. This paper focuses on the friction coefficient, also referred to as frictional strength or simply friction.

This work explores the relationship between friction in granular flows and important physical processes occurring at the grain-scale and macro-scale. Friction in granular materials is known to be strongly rate-dependent. A prime goal is therefore to understand how the various grain-scale and macro-scale processes contribute not only to the absolute value of friction but also to friction's evolution as a function of shear rate. This understanding is important for rapid impact and penetration scenarios, where material strength may evolve significantly throughout the event. Two expressions relating steady state and transient friction to physical processes are derived for shear flows. Numerical simulations using the Discrete Element Method (DEM) [5] are then used to study the scaling behavior of the variables in these relationships. The influence of distinct grain-scale energy dissipation mechanisms on steady state friction is investigated. The future development of new constitutive laws incorporating the derived links will be discussed at the end of the paper.

In past work, simple shear experiments and simulations have been used to establish empirical relationships between steady state friction and shear rate in a granular flow. For instance, in [8] the authors proposed the linear empirical relationship $\mu = a + bI$ for flows of 2D grains, where *a* and *b* are empirical constants and *I* is a non-dimensional shear rate to be described in section 2.1. In [9] the authors proposed the nonlinear empirical relationship $\mu = \mu_0 - (\mu_0 - \mu_1)/(I_0/I + 1)$ for flows of 3D grains, where μ_0, μ_1, and I_0 are empirical constants. The latter relationship has been validated against experiments [9] and used in a rate-dependent constitutive law for field-scale simulations of planetary asteroid impact [4]. Despite the success of these empirical relations, including friction laws incorporating physical processes and material properties into constitutive laws remains a challenge.

Some understanding of the physical processes giving rise to frictional rate-dependence has been found in studies on inertial granular flows. Inertial flows are characterized by a dense packing of grains and an inertial number *I* ($I = \dot{\gamma} d/\sqrt{P/\rho_g}$) between 0.001 and 1. The inertial flow regime is characterized by a marked rate-dependence of steady-state frictional strength and dramatic changes in the internal structure of the material [10]. Most significantly, [8,10] have shown that the anisotropy of the contact force network between grains changes in the inertial flow regime and is directly related to frictional shear strength in the granular flow. This finding provides insight into the microstructural response of the material necessary to resist certain macroscopic loads. In this paper, alternative interpretations of frictional strength and its dependence on shear rate are provided. The inertial flow regime is the primary focus of this paper since, as defined by the inertial number, it is relevant to very rapid impact and shear events (strains up to 10^5 for sub-millimeter sand grains subjected to pressures in the 10s of MPa).

2. Friction Relationships for Granular Shear Flows

2.1. The Inertial Number

An important dimensionless measure of shear rate in granular flows is the inertial number

$$I = \frac{\dot{\gamma} d}{\sqrt{P/\rho_g}} \tag{1}$$

The inertial number can be interpreted to be the ratio of two time scales: a confinement timescale $T_c = d/\sqrt{P/\rho_g}$ proportional to the time required to fully compact a grain after it dilates past its neighbor during the shearing process, and a macroscopic shear timescale $T_\gamma = 1/\dot{\gamma}$ related to the frequency at which a grain is forced past its neighbors. In simple shear flows, $\dot{\gamma}$ is the shear rate in the direction of flow and *P* is the confining stress. In general 3D flows, $\dot{\gamma}$ is replaced by $|\dot{\boldsymbol{\gamma}}|$, the

second invariant of the strain rate tensor, and $P = \gamma_{ii}/3$ is the isotropic pressure. The inertial number is used during the derivation of the two friction relationships, which now follows.

2.2. Friction Relationship for Steady State Shear Flows

A steady state friction relationship can be derived for a granular shear flow (see Fig. 1a) by considering an energy balance equation

$$\frac{\mathrm{d}}{\mathrm{d}t}(T+U) = D_{ij}\gamma_{ji} - \Gamma \tag{2}$$

where T and U are the kinetic and potential energy densities, respectively, $D_{ij}=\partial v_i/\partial x_j$ is the velocity gradient tensor, and Γ is the dissipation rate per unit volume in the material. In steady state simple shear, only one component of the velocity gradient tensor is non-zero ($D_{xy} = \dot{\gamma}$) and the left hand side of Eq. (1) is zero when both sides are time-averaged, yielding

$$\overline{\dot{\gamma}\sigma_{yx}} = \overline{\gamma} \tag{3}$$

where the bars indicate a time average. Defining friction to be $\mu = \bar{\sigma}_{yx}/\bar{\sigma}_{yy}$, assuming all dissipation to occur at grain contact points, and neglecting correlations in the fluctuations of the terms in Eq. (3), the expression becomes

$$\mu = \frac{N_c\langle\Gamma_c\rangle}{\sigma_{yy}\dot{\gamma}V} \tag{4}$$

where all quantities should be assumed to be averaged unless otherwise specified. The act of neglecting correlations in the fluctuations of the terms in Eq. (3) is justified by simulation results, which demonstrate correlations to be negligible. In Eq. (4), N_c is the number of inter-particle contact points in the system, V is the volume of the system, $\langle\Gamma_c\rangle$ is the average per-contact dissipation rate, and the identity $\sum_c^{N_c}\Gamma_c = N_c\langle\Gamma_c\rangle$ has been used. Eq. (4) is simplified by noting that: (1) $N_c = ZN_p/2$ where Z is the coordination number and N_p is the number of particles in the system; (2) the characteristic grain diameter d in the inertial number can be defined such that $N_p(4/3)\pi d^3/8 = V_s$, where V_s is the volume of solids; (3) $V_s/V = \phi$ where ϕ is the solid fraction. These simplifications yield

$$\mu = \frac{Z\phi}{I}\frac{\langle\Gamma_c\rangle}{\tilde{\Gamma}} \tag{5}$$

where $\tilde{\Gamma} = \pi d^2\sigma_{yy}^{3/2}/(3\sqrt{P_g})$ is a pressure-dependent characteristic work rate, a constant for constant-pressure experiments.

Equation (5) is a new relationship between steady state friction in a granular shear flow, solid fraction, coordination number, shear rate, and grain-scale dissipation rates. Shearing dilation, a process by which a granular material reaches a less compact state with a higher solid fraction at higher steady state shear rates, leads to an decrease in coordination number, solid fraction, and therefore $Z\phi/I$ in Eq. (5). However, the increasing shear rates that induce shearing dilation also increase the average dissipation rate at a grain contact point $\langle\Gamma_c\rangle$. Thus, rate-dependence of frictional strength is dictated by a competition between shearing dilation and grain-scale dissipation rates, each of which have opposing effects on friction as seen in Eq. (5).

2.3. Relationship for Transient Shear Flows

Beginning with the energy balance in Eq. (2), a relationship for the transient evolution of friction can be derived, yielding

$$\mu = \frac{Z\phi}{I}\frac{\langle\Gamma_c\rangle}{\tilde{\Gamma}} + \frac{1}{I\tilde{\Gamma}}\frac{d}{dt}(Z\phi\langle U_c\rangle + 2\phi\langle T_p\rangle) + \beta \tag{6}$$

where $\langle U_c\rangle$ is the average stored energy (assumed to be stored as elastic energy at contact points), $\langle T_p\rangle$ is the average kinetic energy of the particles, and $\beta = \dot{\epsilon}_{yy}/\dot{\gamma}$ is the rate of dilatation. The first term in Eq. (6) can be thought of as a steady state term μ_{ss} and the second as a transient energy term μ_t.

Equation (6) is a new relationship for the evolution of friction in non-steady flows. It is similar to Eq. (5), but includes terms involving rate of dilatation and changes in internal energy of the system. It is seen from this expression that a positive

rate of change in internal energy or a positive rate of dilatation invoke an increase in the shear resistance of the material. Equation (6) is similar in form to friction laws proposed in the soil mechanics literature [11,12] which are composed of a steady-state portion and a dilatation portion (e.g. $\mu = \mu_{ss} + \beta$), except that it contains an additional energy term μ_t. In the following section, DEM simulations illustrate how the quantities in Eqs. (5) and (6) evolve with shear rate and material properties and give rise to some of the observed behaviors of frictional strength in granular materials.

3. Numerical Simulations

3.1. Discrete Element Modeling Code

A DEM code is used to study the influence of particle properties and shear rate on the variables in Eqs. (5) and (6). The code is a modified version of the molecular dynamics code LAMMPS. Grains are modelled as spheres and interact with a Hertz-Mindlin contact law described in [13]. The contact model ignores effects of grain fracture and melting and can therefore only be assumed to give an approximation of the true physics of rapidly sheared systems. The simulations discussed here involve spherical grains with 20% bidispersity in diameter that are sheared with periodic *x* and *y* boundary conditions (see Fig. 1a). The grains are sheared between rough walls composed of grains fixed to move together. The parameters held constant during all simulations include the confining pressure, which is chosen in conjunction with the grain stiffness (normal spring constant) to ensure fairly "rigid" grains as discussed in [8]. The confining pressure is held constant by moving the rough walls in the *y* direction as required. The parameters varied throughout the simulations include the grain damping coefficient, chosen to produce a collision-velocity-dependent coefficient of restitution ϵ, and an inter-particle friction coefficient μ_p that restricts the ratio of the tangential mechanical force to the normal mechanical force at a contact before truncation of the tangential force. The three data sets investigated are detailed in Fig. 1c.

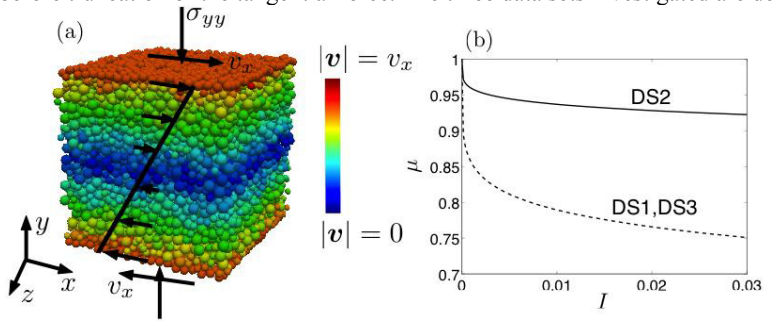

(c)

Data Set	μ_p	e
DS1	0.3	-- in Fig 1b
DS2	0.3	- in Fig 1b
DS3	0.6	-- in Fig 1b

Figure 1 – (a) Illustration of simple shear flow simulation. (b) Illustration of coefficient of restitution used in the three data sets. (c) Quantities used for material properties in the three data sets. The description of coefficient of restitution in (c) relates to the curves in (b).

3.2. Steady State Simulations

Steady state simple shear flows are investigated by running simulations until a steady state is reached in the time-averages of all quantities in Eq. (5). The averaged quantities are used to compute Eq. (5). The result is compared to the equation for friction $\mu = \bar{\sigma}_{yx}/\bar{\sigma}_{yy}$, where the stress components are computed using the coarse-graining expression [14]

$$\sigma_{ij} = \frac{1}{V}\sum_{c=1}^{N_c} l_i^c \otimes f_j^c \tag{7}$$

where l_i^c is a vector pointing from the centroid of particle *j* to the centroid of *i*, f_i^c is a contact force from particle *j* to *i*, and $\otimes$ is a dyadic (tensor) product. The resulting comparison for all the three data sets investigated here is shown in Fig. 2a. An excellent agreement is seen for each data set in Fig. 2a, indicating that Eq. (5) accurately links friction to important processes such as shearing dilation and grain-scale dissipation processes.

A decomposition of Eq. (5) into two components $\mu = \mu_n + \mu_s$, one furnished by viscoelastic processes with the other furnished by grain-sliding, can be derived by considering the contact law described in section 3.1. Letting $\langle \Gamma_n \rangle$ be the average per-contact energy dissipation rate by viscoelastic processes within the grains and $\langle \Gamma_s \rangle$ to be the average per-contact energy dissipation rate at grains sliding past surrounding grains, the two components in the decomposition can be written as

$$\mu_s = \frac{Z\phi\langle\Gamma_n\rangle}{I\tilde{\Gamma}} \quad \text{and} \quad \mu_s = \frac{Z\phi\langle\Gamma_s\rangle}{I\tilde{\Gamma}} \tag{8}$$

An illustration of the evolution of each of these terms is given in Fig. 2b. For all data sets, grain sliding furnishes all of the granular material's frictional strength at low shear rates. As shear rates increase, the viscoelastic energy dissipation mechanism contributes increasingly to frictional strength. For DS1, the viscoelastic contribution increases rapidly, overtaking the grain-sliding contribution at approximately I=0.62. For DS2, which features a higher coefficient of restitution for the grains, the viscoelastic contribution never overtakes the grain-sliding contribution. This is likely because less energy is dissipated due to viscoelasticity in each collision, causing higher impact velocities and leading more energy to be dissipated through grain sliding. For DS3, the viscoelastic contribution and grain sliding contribution are very similar to those of DS1, except that the viscoelastic contribution overtakes the grain-sliding contribution at a lower shear rate, around I=0.55. Interestingly, both DS1 and DS3 feature very similar behaviors in Figs. 2a and 2b. The increased inter-particle friction coefficient in DS3 only appears to shift the total friction curve upward (see Fig. 2a) but does not change its general shape. Hence, it seems that changing the slope of the $\mu(I)$ curve at a given shear rate is primarily accomplished by varying the restitution coefficient of the grains. This finding is supported by other work that finds a transition from rate-dependent inertial flows to rate-independent gas-like rapid flows to be determined mainly by the coefficient of restitution [15].

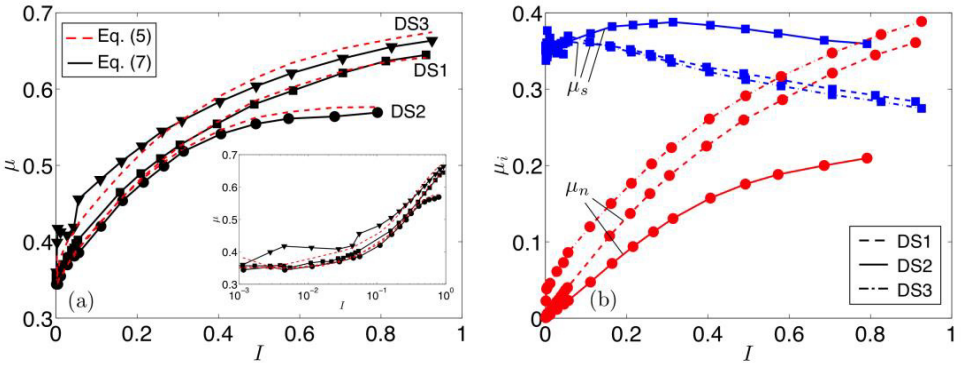

Figure 2 – (a) Comparison of the friction coefficients computed using Eq. (5) (dashed red curves) with those computed using Eq. (7) (solid black curves with symbols) for each of the three data sets. The inset shows the same data with a logarithmic scale for shear rate, illustrating the onset of rate-dependence in the inertial flow regime. (b) Evolution of distinct grain-scale contributions to macroscopic friction for each data set. Error bars are not shown for either figure to improve readability. However, error bars marking one standard deviation on each friction measurement are typically span less than 0.05 from the shown data points.

Figure 3 illustrates the evolution of the components in Eq. (5) as a function of shear rate for the three data sets investigated. The finding indicates that shearing dilation and grain-scale dissipation rates play competing roles in determining the strength of a sheared granular material. Shearing dilation decreases the internal area over which energy can be dissipated by decreasing the coordination number Z and the solid fraction ϕ. Simultaneously, grain-scale dissipation rates increase with shear rates due to higher grain collision velocities and inter-particle forces, increasing $\langle\Gamma_c\rangle/\langle\tilde{\Gamma}\rangle$.

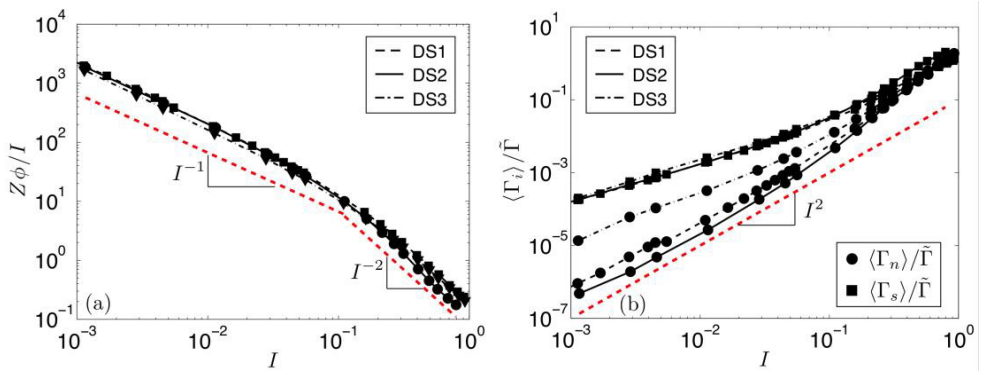

Figure 3 – (a) Evolution of the term $Z\phi/I$ shows two distinct scaling regimes in the inertial flow regime. (b) Dissipation rate terms scale close to I^2 for $\langle\Gamma_s\rangle/\langle\tilde{\Gamma}\rangle$ and faster than I^2 for $\langle\Gamma_n\rangle/\langle\tilde{\Gamma}\rangle$.

The term $Z\phi/I$ shown in Fig. 3a has two distinct scaling behaviors in the inertial flow regime. All data sets appear to collapse onto the scaling $Z\phi/I \propto I^{-1}$ at low shear rates, consistent with the fact that Z and ϕ maintain maximum quasi-static values at low shear rates. Similarly, all data sets collapse onto the scaling $Z\phi/I \propto I^{-2}$ at high shear rates due to a decrease in Z and ϕ. The transition between these two behaviors occurs at a shear rate (I=0.1) at which dramatic changes in internal structure of the material have been observed to occur [10]. The energy dissipation rate terms in Fig. 3b also have a characteristic scaling behavior close to I^2 for $\langle\Gamma_s\rangle/\langle\tilde{\Gamma}\rangle$ and faster than I^2 for $\langle\Gamma_n\rangle/\langle\tilde{\Gamma}\rangle$. The latter scaling can be derived from the fact that collision velocities scale with the inertial number and the contact law requires viscous forces to scale with collision velocities. When combined, the competing scaling of $Z\phi/I$ and $\langle\Gamma_n\rangle/\langle\tilde{\Gamma}\rangle$ observed in these simulations gives rise to the rate-strengthening of the friction coefficient shown in Fig. 2a. This is a common feature of inertial flows seen in the literature [8-11] and used in modelling of rapid impact events [4]. From the preceding analysis, it is understood to arise because grain-scale dissipation rates increase faster with shear rate than dilation-induced quantities $Z\phi/I$ decrease.

3.3. Transient Simulations

The transient simple shear flow simulations are performed only with grain properties used in DS1 above. The simulations are performed as follows. First, a confining pressure is applied to the simple shear flow configuration shown in Fig. 1a. A slow shear rate (I=0.001) is then applied to the material to allow quasi-static values of Z and ϕ to be reached. Once a steady-state is reached at the slow shear rate, a faster shear rate (I=0.5) is instantaneously applied to the material by changing the velocity of the boundaries. The boundaries are allowed to expand in the y direction while the material seeks vertical stress equilibrium. The boundaries are given mass equal to ten times the sum of the masses of the particles that compose them. A small global damping parameter is used to prevent the boundary from accelerating upward too quickly or oscillating while the material seeks vertical stress equilibrium [5]. The mass of the boundaries has a minimal effect on the rate at which the material reaches a new equilibrium. The damping parameter has an influence on the rate at which the material reaches a new equilibrium, but is chosen to be the smallest value below which a damping parameter would allow the boundaries to oscillate.

Variables in Eq. (6) are monitored in a thin layer of grains within the flow to ensure the shear rate is uniform (see Fig 4a). Only one layer is analysed in this work for brevity. Considering the assembly as a whole is not appropriate since the flow profile evolves according to a momentum-diffusion type process, making the full flow profile non-linear and invalidating the homogeneous shear rate required in the inertial number. The evolutions of spatially averaged quantities in Eq. (6) are therefore averaged over fewer than the total 10,000 modelled grains and possess considerably more variability than in the steady state case. Some variables are fit with a smooth curve before being used in Eq. (6), as discussed in Appendix A.

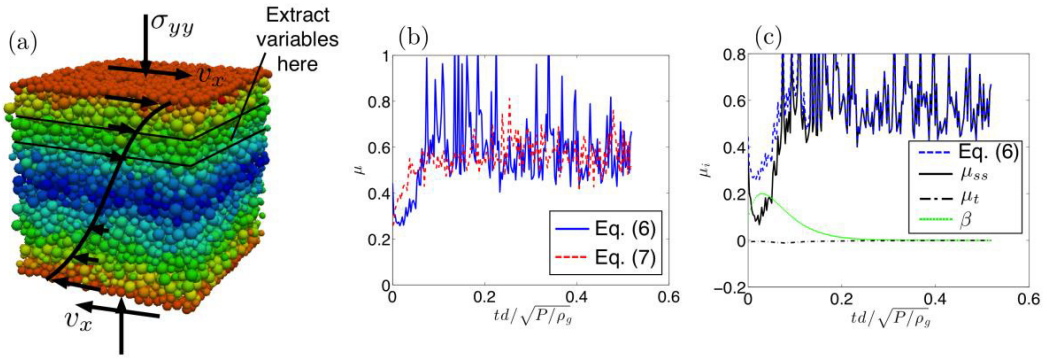

Figure 4 – (a) Location of region where variables in Eq. (6) were extracted to compute the transient evolution of the friction coefficient. Grain colors are the same as those in Fig. 1a. (b) Comparison of the transient friction coefficient in the specified layer computed using the proposed friction law (Eq. (6), solid blue curve) and the coarse-grained stress formula (Eq. (7), dashed red curve). (c) Comparison of the three terms in Eq. (6). The steady-state term (solid black line) evolves slowly to the its new value while the rate of dilatation (dotted green curve) provides part of the transient frictional response at early times while the transient energy term (dot-dashed black curve) is negligible at all times.

Figure 4b shows the evolution of the friction coefficient in the layer of interest computed using the friction relationship in Eq. (6) and the coarse-graining expression in Eq. (7). The time t=0 corresponds to the time at which the velocity step is applied to the boundaries. The friction relationship in Eq. (6) is seen to provide a decent estimate of the friction coefficient as a function of time. The major difference is the slight offset of the curves at early times and the large variability in the curve computed using Eq. (6).

Figure 4c shows the evolution of the 3 terms in Eq. (6) with time. At early times, the steady state term (first term in Eq. (6)) decreases due to an increase in the confining pressure in the layer (e.g., an increase in $I\tilde{\Gamma}$). The rate of dilatation β (third term in Eq. (6)) partially compensates for this decrease, increasing rapidly before quickly decaying to zero. The transient energy term (second term in Eq. (6)) is negligible for the entire simulation. Remarkably, this suggests that the transient evolution of friction in some rapid shear flows is similar in nature to the observed evolution of friction in soil mechanics [11,12]. More work is needed to determine how this behavior changes in simulations employing other material properties or shear rates.

4. Discussion and Future Work

The theoretical relationships derived in section 2 provide a link between frictional strength and the physical processes occurring in inertial granular flows. The relationships also provide insight into the influence of grain properties on frictional strength. Figure 2 illustrated that grain properties related to the restitution coefficient (e.g. the Young's modulus and plasticity law of the bulk grain material) contribute more to shaping frictional rate-dependence than inter-particle friction coefficient of the grains. Additional simulations are needed to investigate the influence of grain shape on frictional strength and rate-dependence in granular shear flows. Additional work is also needed to extend Eqs. (5) and (6) to include the effects of additional physics, such as grain fragmentation and melting, that may influence a granular material's response in certain rapid shearing and impact events.

A prime future goal of this work is to foster the development of constitutive laws for continuum modelling of rapid shear flows and impact events. Some preliminary work has been done on incorporating Eqs. (5) and (6) into the constitutive laws developed in [9]. For instance, using the stress tensor decomposition proposed in [9] and a derivation similar to that for Eq. (4), the stress tensor in a granular material undergoing a general 3D steady state deformation can be written as

$$\sigma_{ij} = P\left(-\delta_{ij} + \frac{Z\phi\langle\Gamma_c\rangle}{I\tilde{\Gamma}}\frac{\dot{\gamma}_{ij}}{|\dot{\boldsymbol{\gamma}}|}\right) \tag{9}$$

Equation (9) can be used in continuum numerical simulations with an appropriate equation of state relating P to ϕ and equations governing the evolution of coordination number Z and grain-scale dissipation rates $\langle\Gamma_c\rangle$. The influence of grain properties can be incorporated into evolution laws for Z and $\langle\Gamma_c\rangle$ to create a physics-based constitutive law suitable for field-scale simulations. It may be possible to simulate non-steady flows with Eq. (9) if the response on short time scales like those seen in Fig. 4c is not needed. This is the subject of on-going research.

The simulations probing the transient behavior of friction reveal that, in certain flows, friction has the simple form $\mu = \mu_{ss} + \beta$, as in soil mechanics [11,12]. However, more work is needed to understand the influence of shear rates and

grain properties. The present results merely illustrate the accuracy of Eq. (6). There may be material properties or shear rates for which the transient energy term μ_t is not negligible as it was in the simulations shown in Fig. 4. Considering thermal effects in simulations may also significantly alter the contribution of each term in the expression.

5. Conclusion

This work examines the physical processes underlying frictional strength in flowing granular media. Such processes are crucial to understanding and accurately modelling rapid deformation and impact events. Relationships linking steady state and transient frictional strength to properties such as coordination number, solid fraction, shear rate, rate of dilatation, and the rate of change in internal energy have been derived. The steady state expression illustrates the competing mechanisms governing steady state frictional rate-dependence: shearing dilation and grain-scale dissipation rates. The transient friction relationship illustrates that the evolution of strength during transient loading is influenced explicitly by the rate of dilatation and by rates of change in the internal energy of the material. Simulations shown here indicate that the rates of change in the internal energy of the material are negligible for certain grain properties and shear rates.

The intended consequence of the current work is to facilitate the development of constitutive laws that can improve the physical accuracy and predictive capacity of numerical simulations. On-going and future work will continue to investigate the friction laws proposed here and their role in constitutive laws.

Acknowledgements

Support from the Air Force Office of Scientific Research Grant #FA9550-12-1-0091 through the University Center of Excellence in High-Rate Deformation Physics of Heterogeneous Materials is gratefully acknowledged.

References

[1] Jaeger, H. M., Nagel, S. R., Behringer, R. P., 1996. Granular solids, liquids, and gases. Reviews of Modern Physics, 68(4), 1259.
[2] Omidvar, M., Iskander, M., Bless, S., 2014. Response of granular media to rapid penetration. International Journal of Impact Engineering, 66, 60-82.
[3] Luo, H., Chen, W. W., & Rajendran, A. M., 2006. Dynamic Compressive Response of Damaged and Interlocked SiC–N Ceramics. Journal of the American Ceramic Society, 89(1), 266-273.
[4] Jutzi, M., Asphaug, E., 2011. Forming the lunar farside highlands by accretion of a companion moon. Nature, 476(7358), 69-72.
[5] Cundall, P. A., Strack, O. D., 1979. A discrete numerical model for granular assemblies. Geotechnique, 29(1), 47-65.
[6] Tang, Z. P., Horie, Y., Psakhie, S. G., 1996. Discrete meso-element dynamic simulation of shock response of reactive porous solids. In American Institute of Physics Conference Series (Vol. 370, pp. 657-660).
[7] Savage, S. B., 1984. The mechanics of rapid granular flows. Advances in applied mechanics, 24, 289-366.
[8] da Cruz, F., Emam, S., Prochnow, M., Roux, J. N., Chevoir, F., 2005. Rheophysics of dense granular materials: Discrete simulation of plane shear flows. Physical Review E, 72(2), 021309.
[9] Jop, P., Forterre, Y., Pouliquen, O., 2006. A constitutive law for dense granular flows. Nature, 441(7094), 727-730.
[10] Azéma, E., Radjaï, F., 2014. Internal structure of inertial granular flows. Physical review letters, 112(7), 078001.
[11] Andrade, J. E., Chen, Q., Le, P. H., Avila, C. F., Matthew Evans, T., 2012. On the rheology of dilative granular media: Bridging solid-and fluid-like behavior. Journal of the Mechanics and Physics of Solids, 60(6), 1122-1136.
[12] Wood, D. M., 1990. Soil behavior and critical state soil mechanics. Cambridge university press.
[13] http://lammps.sandia.gov/doc/pair_gran.html
[14] Bagi, K., 1996. Stress and strain in granular assemblies. Mechanics of materials, 22(3), 165-177.
[15] Forterre, Y., Pouliquen, O. 2008. Flows of dense granular media. Annu. Rev. Fluid Mech., 40, 1-24.

Appendix A – Curve Fitting in Transient Simulations

Smooth curves are fit to some of the variables extracted for analysis of Eq. (6). Fitting is achieved using least squares curves fits in MATLAB. In particular, a smooth curve is fit to the rate of dilatation term β of the form proposed in [11]

$$\beta = \beta^* \frac{t}{t^*} \exp\left(1 - \frac{t}{t^*}\right) \tag{10}$$

where asterisks indicate fitting parameters. Similarly, a smooth curve of the following form is fit to the quantity $Z\phi\langle U_c\rangle + 2\phi\langle T_p\rangle$ and its derivative was subsequently found analytically

$$f = a^* + \frac{b^* - a^*}{t^*/t + 1} \tag{11}$$

These fits are necessary to make the presentation of the results in Figs. 4b and 4c clear. Without the fitting, large oscillations dominate these figures. General trends in all fitted quantities are not significantly changed in the fitting process.